论著·基础医学

S100a6通过β-catenin/TCF1依赖性转录抑制调控PARP9/STAT1改善冠状动脉微循环障碍

刘 春[1],杨清媛[1],邓忠芳[1],蔡筱诗[1],赖晓玥[2],陈 铭[1],万小勤[1],汪紫阳[1],郑 攀[1],邓 芳[3],张志辉[1] [1]陆军军医大学(第三军医大学)第一附属医院心血管内科,代谢生物钟与心血管疾病中心,老年心脑血管病教育部重点实验室,重庆;[2]陆军军医大学(第三军医大学)第二附属医院超声医学科,重庆;[3]陆军军医大学(第三军医大学)高原军事医学系病理生理学教研室,重庆

[**摘要**] **目的** 冠状动脉微循环障碍(coronary microvascular dysfunction, CMD)在冠心病群体中患病率高,且作为独立危险因素大幅增加心血管事件风险,但缺乏靶向干预措施。钙周期蛋白(S100a6)具有调节内皮细胞周期的作用,但其在CMD中的表达特征及保护机制尚不明确。本研究旨在明确S100a6在CMD中的内源性保护作用,阐明其通过稳定β-catenin/TCF1复合体抑制PARP9/STAT1信号轴活化改善CMD的分子机制。**方法** 选用8周龄、体质量38~42 g的雄性ob/ob小鼠共12只,采用随机数字表法将小鼠分为CMD组与CMD-S100a6KD组(n=6)。其中,CMD组小鼠经尾静脉注射scramble对照病毒,CMD-S100a6KD组小鼠经尾静脉注射内皮特异性的腺病毒以敲低S100a6的表达。另选取6只同周龄的雄性C57BL/6J野生型小鼠(体质量18~22 g)作为健康对照组(Control组),常规饲养不做任何模型构建及药物或基因干预。通过尾静脉注射内皮特异性Tie启动子驱动的AAV9-shS100a6实现S100a6内皮特异性敲低,20周后通过心脏超声检测小鼠冠状动脉血流储备(coronary flow reserve, CFR)及左心室舒张功能(E/e′),取小鼠心脏组织行免疫荧光染色检测心肌微血管密度及相关蛋白表达与定位。体外培养人冠状动脉微血管内皮细胞(human coronary microvascular endothelial cells, HCMECs),以高糖(25 mmol/L)联合游离脂肪酸(0.5 mmol/L)处理48 h构建CMD细胞模型,采用siRNA及质粒进行基因干预。根据不同实验目的分为:基线对照组[正常培养的对照组(Control组)和CMD模型组(HG组)]、S100a6功能缺失组(HG+siS100a6和HG+siNC组)及下游机制挽救组(HG+siS100a6+siPARP9及其HG+siS100a6+siNC组、HG+siS100a6+OE β-catenin及其HG+siS100a6+OE NC组)。通过单细胞RNA测序分析心脏组织S100a6的细胞亚群表达,并通过批量RNA测序筛选差异基因与富集通路;以Western blotting、RT-qPCR检测S100a6、β-catenin、TCF1、PARP9、STAT1及p-STAT1的蛋白相对表达量与mRNA表达水平;采用免疫共沉淀方法验证β-catenin与TCF1相互作用,通过染色质免疫共沉淀方法检测TCF1与PARP9启动子结合能力,明确相关分子机制。通过EdU增殖实验、划痕愈合实验及成管实验评估内皮细胞功能。**结果** 与CMD组比较,CMD-S100a6KD组小鼠CFR显著降低(P<0.05),E/e′比值显著升高(P<0.05),心肌微血管密度显著降低(P<0.05)。单细胞RNA测序结果显示,CMD组小鼠心脏组织中S100a6整体表达显著升高,且在心脏内皮细胞亚群中显著升高(P<0.05);免疫荧光共定位分析显示S100a6与CD31的共定位信号明显增强(P<0.000 1)。体外实验中,高糖高脂刺激使HCMECs

[**基金项目**] 国家自然科学基金面上项目(82570409);重庆市技术创新与应用发展专项重点项目(CSTB2023TIAD-KPX0061-2)

[**通信作者**] 邓 芳,E-mail:celldf@tmmu.edu.cn

张志辉,E-mail:xyzpj@tmmu.edu.cn

2097-0927/Copyright © 2026, 陆军军医大学(第三军医大学)。这篇开放获取文章遵循CC BY许可协议(https://creativecommons.org/licenses/by/4.0/)

引用格式:刘春,杨清媛,邓忠芳,等.S100a6通过β-catenin/TCF1依赖性转录抑制调控PARP9/STAT1改善冠状动脉微循环障碍[J].陆军军医大学学报,2026,48(10):1368-1382. DOI:10.16016/j.2097-0927.202602088.

Citation:LIU C, YANG Q Y, DENG Z F, *et al*. S100a6 ameliorates coronary microcirculatory dysfunction by modulating PARP9/STAT1 *via* β-catenin/TCF1-dependent transcriptional repression[J]. J Army Med Univ, 2026, 48(10):1368-1382. DOI:10.16016/j.2097-0927.202602088.

S100a6蛋白表达水平显著高于正常培养的对照组($P<0.05$)。S100a6敲低导致HCMECs成管分支数显著减少($P<0.05$)、划痕愈合率显著降低($P<0.05$)及EdU阳性率显著降低($P<0.05$)。批量RNA测序结果显示S100a6敲低后*PARP9*基因表达显著上调,基因富集分析显示STAT1信号通路显著富集;在敲低S100a6的同时敲低PARP9,STAT1磷酸化水平较单纯S100a6敲低组显著降低($P<0.000\ 1$);功能学实验证实沉默PARP9显著改善了S100a6敲低引起的HCMECs成管功能障碍($P<0.05$)、迁移能力受损($P<0.05$)及EdU阳性率降低($P<0.05$)。分子对接实验显示S100a6结合在TCF1和β-catenin的结合界面缝隙中;敲低S100a6使β-catenin蛋白水平显著降低($P<0.05$),β-catenin与TCF1的相互作用显著减弱($P<0.05$),TCF1与*PARP9*启动子区域的结合显著减少($P<0.05$)。在敲低S100a6的同时过表达β-catenin使PARP9蛋白表达水平显著降低($P<0.05$),磷酸化STAT1水平显著下降($P<0.05$);功能学层面,β-catenin过表达显著改善了S100a6缺失导致的HCMECs成管分支数减少($P<0.05$)、划痕愈合率降低($P<0.05$)及EdU阳性率降低($P<0.05$)。**结论** S100a6是冠状动脉微循环障碍的内源性保护因子,其通过β-catenin/TCF1复合体依赖性转录抑制调控PARP9/STAT1信号通路的活化,维持内皮细胞稳态,进而改善冠状动脉微循环障碍。

[**关键词**] 冠状动脉微循环障碍;内皮细胞功能障碍;S100a6;β-连环蛋白;多聚(ADP-核糖)聚合酶9

[**中图法分类号**] R341;R394.3;R543.3 [**文献标志码**] A

S100a6 ameliorates coronary microcirculatory dysfunction by modulating PARP9/STAT1 *via* β-catenin/TCF1-dependent transcriptional repression

LIU Chun[1], YANG Qingyuan[1], DENG Zhongfang[1], CAI Xiaoshi[1], LAI Xiaoyue[2], CHEN Ming[1], WAN Xiaoqin[1], WANG Ziyang[1], ZHENG Pan[1], DENG Fang[3], ZHANG Zhihui[1] [1]Department of Cardiology, Center for Metabolic Circadian Clock and Cardiovascular Diseases, Key Laboratory of Geriatric Cardio-Cerebrovascular Disease of Ministry of Education First Affiliated Hospital, Army Medical University (Third Military Medical University), Chongqing; [2]Department of Ultrasonography, Second Affiliated Hospital, Army Medical University (Third Military Medical University), Chongqing; [3]Department of Pathophysiology, College of High Altitude Military Medicine, Army Medical University (Third Military Medical University), Chongqing, China

[**Abstract**] **Objective** Coronary microvascular dysfunction (CMD) is highly prevalent among patients with coronary artery disease and, as an independent risk factor, increases the risk of cardiovascular events, yet there is a lack of targeted interventions. S100a6 has been shown to regulate endothelial cell cycle progression, but its expression pattern and protective mechanism in CMD remain unclear. This study aimed to determine the endogenous protective role of S100a6 in CMD and to elucidate the molecular mechanism by which it ameliorates CMD through stabilizing the β-catenin/TCF1 complex and suppressing the activation of the PARP9/STAT1 signaling axis. **Methods** A total of 12 male ob/ob mice, aged 8 weeks and weighing 38 to 42 g, were randomly assigned into 2 groups (n=6 per group) using a random number table: the CMD group and the CMD-S100a6KD group. Mice in the CMD group received injection *via* tail vein of scrambled control virus, whereas those in the CMD-S100a6KD group received endothelium-specific adenovirus to knock down S100a6 expression. Additionally, six male C57BL/6J wild-type mice of the same age, weighing 18 to 22 g, were used as a healthy control group (Control group) and were fed routinely without any model construction or drug/gene intervention. Endothelial-specific knockdown of S100a6 was achieved by tail vein injection of AAV9-shS100a6 driven by an endothelium-specific Tie promoter. After 20 weeks, coronary flow reserve (CFR) and left ventricular diastolic function (E/e′) were assessed by echocardiography; heart tissues were collected for immunofluorescence staining to evaluate myocardial microvessel density and related protein expression and

localization. Human coronary microvascular endothelial cells (HCMECs) were cultured in vitro and treated with high glucose (25 mmol/L) combined with free fatty acids (0.5 mmol/L) for 48 h to establish a CMD cell model, followed by gene intervention using siRNA and plasmids. Experimental groups were designed according to different objectives: baseline control groups [the normal culture control group (Control group) and the CMD model group (HG group)], S100a6 loss-of-function groups (HG+siS100a6 and its siNC control), and downstream mechanism rescue groups (HG+siS100a6+siPARP9 and its siNC control; HG+siS100a6+OE-β-catenin and its empty vector control). Single-cell RNA sequencing was used to analyze the cell-subset expression of S100a6 in heart tissues, and bulk RNA sequencing was performed to identify differentially expressed genes and enriched pathways. Western blotting and qRT-PCR were used to measure the relative protein and mRNA expression levels of S100a6, β-catenin, TCF1, PARP9, STAT1, and p-STAT1. Co-immunoprecipitation was performed to validate the interaction between β-catenin and TCF1, and chromatin immunoprecipitation was used to detect the binding of TCF1 to the PARP9 promoter, thereby clarifying the molecular mechanism. Endothelial cell function was assessed by EdU proliferation assay, scratch wound healing assay, and tube formation assay. **Results** Compared with the CMD group, mice in the CMD-S100a6KD group showed a significantly reduced CFR ($P<0.05$), a significantly increased E/e' ratio ($P<0.05$), and a significantly decreased myocardial microvessel density ($P<0.05$). Single-cell RNA sequencing revealed that S100a6 expression was markedly elevated overall in the heart tissues of CMD group mice, and it is also significantly upregulated in the subsets of cardiac endothelial cells ($P<0.05$); immunofluorescence co-localization analysis showed significantly enhanced co-localization signals of S100a6 and CD31 ($P<0.000\ 1$). *In vitro*, high glucose and high lipid stimulation significantly increased S100a6 protein expression levels in HCMECs compared with normally cultured controls ($P<0.05$). Knockdown of S100a6 led to a significant reduction in the number of tube branches ($P<0.05$), a significant decrease in scratch wound healing rate ($P<0.05$), and a significant decrease in EdU-positive rate ($P<0.05$) in HCMECs. Bulk RNA sequencing showed that PARP9 gene expression was significantly upregulated after S100a6 knockdown, and gene enrichment analysis revealed significant enrichment of the STAT1 signaling pathway. When S100a6 and PARP9 were knocked down simultaneously, STAT1 phosphorylation levels were significantly reduced compared with the S100a6 knockdown alone group ($P<0.000\ 1$). Functional assays confirmed that PARP9 silencing significantly ameliorated the S100a6 knockdown-induced impairments in tube formation ($P<0.05$), migration capacity ($P<0.05$), and EdU-positive rate ($P<0.05$) in HCMECs. Molecular docking experiments showed that S100a6 binds within the crevice of the TCF1/β-catenin interaction interface. Knockdown of S100a6 significantly reduced β-catenin protein levels ($P<0.05$), significantly weakened the interaction between β-catenin and TCF1 ($P<0.05$), and significantly decreased the binding of TCF1 to the PARP9 promoter region ($P<0.05$). Overexpression of β-catenin in parallel with S100a6 knockdown significantly reduced PARP9 protein expression levels ($P<0.05$) and reduced phosphorylated STAT1 levels ($P<0.05$). Functionally, β-catenin overexpression significantly rescued the S100a6 deficiency-induced reductions in tube branch number ($P<0.05$), scratch wound healing rate ($P<0.05$), and EdU-positive rate ($P<0.05$) in HCMECs. **Conclusion** S100a6 is an endogenous protective factor for coronary microcirculatory dysfunction. It regulates the activation of the PARP9/STAT1 signaling pathway through β-catenin/TCF1 complex-dependent transcriptional repression, maintains endothelial cell homeostasis, and thereby ameliorates coronary microcirculatory dysfunction.

[**Key words**] coronary microvascular dysfunction; endothelial dysfunction; S100a6; β-catenin; poly(ADP-ribose) polymerase family member 9

Supported by the General Program of National Natural Science Foundation of China (82570409) and the Key Special Project for Technological Innovation and Application Development of Chongqing (CSTB2023TIAD-KPX0061-2). Corresponding authors: DENG Fang, E-mail: celldf@tmmu.edu.cn; ZHANG Zhihui, E-mail: xyzpj@tmmu.edu.cn

冠状动脉疾病(coronary artery disease, CAD)及其并发症是全球范围内导致死亡和伤残的首要原因[1]。冠状动脉微循环障碍(coronary microvascular dysfunction, CMD)是影响CAD患者预后不良的重要危险因素,常独立于梗阻性冠状动脉疾病发生[2-3],提示微血管功能障碍本身即可作为心肌缺血的独立致病机制。内皮细胞功能障碍在CMD的发病机制中具有重要作用[4-5]。在代谢紊乱(如肥胖、胰岛素抵抗)及慢性应激状态下,人冠状动脉微血管内皮细胞(human coronary microvascular endothelial cells, HCMECs)发生表型改变,表现为增殖受阻、迁移能力下降及成管功能缺陷,进而导致微血管密度降低和冠状动脉血流储备(coronary flow reserve, CFR)降低,最终引发心力衰竭[2,6-8]。然而,目前CMD的发病机制仍未阐明,临床亦缺乏针对微血管保护的特异性干预措施[7-8]。因此,深入解析维持微血管内皮稳态的关键分子机制,对于寻找改善CMD的新靶点具有重要的理论意义和临床应用价值。

钙周期蛋白(S100a6)是S100家族的低分子量钙结合蛋白,参与细胞增殖、细胞骨架重组及应激反应等多种细胞过程[9-11]。S100a6在心血管病理中的生物学角色长期存在争议,既往研究多将S100a6视为细胞应激或损伤的标志分子:急性冠脉综合征患者血清S100a6水平升高曾被归因为细胞膜破裂后的蛋白渗漏,是反映组织损伤程度的生物标志物[12]。然而,越来越多的证据提示S100a6可能具有主动保护功能:在心肌细胞中,S100a6可通过调节p53磷酸化状态抑制细胞凋亡,从而减轻缺血再灌注损伤[13]。更重要的是,S100a6被鉴定为内皮细胞周期进程的关键调节因子,其缺失可直接导致内皮细胞增殖停滞[14]。上述研究揭示了S100a6在心血管保护中的潜在价值,但其在代谢性CMD这一特定病理环境下的功能尚未阐明,特别是在代谢紊乱引发的CMD发生发展的进程中,内源性S100a6究竟是损伤的参与者还是代偿性保护因子,尚未被明确界定。本研究通过单细胞RNA测序、ob/ob-CMD小鼠模型验证及体外细胞实验,旨在明确S100a6在CMD中的表达特征及功能,并深入探讨其缺失加重冠状动脉微循环障碍的分子机制,为冠状动脉微血管病的防治提供实验依据和新靶点。

1 材料与方法

1.1 实验动物

基于目前所公认的CMD动物模型[15-17],将12只体质量为38~42 g的8周龄ob/ob雄性小鼠按随机数字表法分为CMD组和CMD-S100a6KD组,每组6只;另取6只体质量18~22 g的8周龄C57BL/6J雄性小鼠作为健康对照组(Control组)。所有小鼠购自常州卡文斯实验动物有限公司,饲养于SPF级动物房,环境温度为(22±2) ℃,相对湿度(50±10)%,采用12 h光照/12 h黑暗周期,自由摄取标准饲料和水。CMD-S100a6KD组和CMD组小鼠通过尾静脉分别注射内皮特异性的腺相关病毒和scramble对照病毒,每只150 μL,病毒滴度≥1×10^{12} vg/mL,Control组常规饲养不做任何模型构建及药物或基因干预。初次注射后6周进行同等剂量加强注射,确保持续基因沉默,在20周时经小鼠腹腔注射1%戊巴比妥钠进行麻醉后取材。本研究设定明确的人道终点(小鼠体质量下降超过20%或出现不可逆呼吸困难)。实验动物的健康状况由专业人员每日早、晚各监测1次,如小鼠达到人道终点,将立即腹腔注射戊巴比妥钠(150 mg/kg)实施安乐死。动物实验均通过陆军军医大学实验动物福利与伦理委员会批准(AMUWE2023970)。

1.2 试剂与仪器

内皮特异性Tie启动子驱动AAV9购自中国汉恒生物科技有限公司;HCMECs购自中国昂羽生物技术有限公司;内皮细胞培养基(endothelial cell medium, ECM)、胎牛血清(fetal bovine serum, FBS)、内皮细胞生长因子(endothelial cell growth supplement, ECGS)及青-链霉素溶液均购自美国ScienCell Research Laboratories公司;GP-transfect-Mate转染试剂及靶向S100a6、PARP9的siRNA购自中国吉玛基因公司;S100a6和β-catenin过表达质粒购自中国汉恒生物科技有限公司;RNA提取试剂盒、反转录体系、SYBR Green qPCR Master Mix均购自中国艾博泰克公司;S100a6抗体、β-catenin抗体、TCF1抗体、PARP9抗体及GAPDH抗体购自中国三鹰公司;STAT1抗体、p-STAT1抗体及SimpleChIP™酶促染色质免疫沉淀试剂盒购自美国Cell Signaling Technology公司;TSA荧光试剂盒购自中国艾方生物公司;EdU细胞增殖检测试剂盒购自中国菲恩生物公司;Matrigel基质胶购自中国白鲨生物技术公司;TRIzol试剂、RIPA裂解液、BCA蛋白定量试剂盒、4%多聚甲醛、Triton X-100及抗荧光淬灭剂购自中国碧云天公司;实时超声诊断仪(VINNO V6, OSEI BIO)购自中国飞依诺科技股份有限公司;激光共聚焦显微镜购自德国蔡司公司。

1.3 细胞培养与处理

HCMECs以ECM培养基为基础,添加5%FBS、1%ECGS及1%青-链霉素溶液,置于37 ℃、5%CO_2恒温

培养环境中常规培养,待细胞生长至合适密度后,给予25 mmol/L高糖联合0.5 mmol/L游离脂肪酸共同刺激并持续培养48 h,构建体外代谢紊乱CMD细胞模型(HG组);随后严格按照制造商说明书,分别转染靶向S100a6、PARP9的小干扰RNA及S100a6、β-catenin过表达质粒。根据实验目的将细胞分为基线对照组(正常培养的Control组、高糖高脂处理的HG组)、S100a6功能缺失组(HG+siS100a6组及其对照HG+siNC组)及下游机制挽救组(HG+siS100a6+siPARP9组及其对照HG+siS100a6+siNC组、HG+siS100a6+OE-β-catenin组及其对照HG+siS100a6+OE-NC组)。

1.4 小鼠心脏组织单细胞RNA测序与高糖高脂处理后HCMECs批量RNA测序

小鼠经戊巴比妥钠(50 mg/kg)麻醉后,取心脏组织,液氮速冻后-80 ℃保存,送至上海派森诺生物科技股份有限公司进行单细胞解离、文库构建,采用10x Genomics Chromium平台测序,Illumina NovaSeq 6000系统测序。原始数据经Cell Ranger处理后,使用Seurat软件进行标准流程分析。收集HG组和HG+siS100a6组HCMECs,TRIzol试剂提取2组总RNA,送至欧易生物科技有限公司进行批量RNA测序,质控后清洁读数比对映射至参考基因组GRCh38/hg38版本,使用DESeq2进行差异基因表达分析。

1.5 小鼠冠状动脉血流储备与心脏舒张功能超声检测

小鼠经1.5%异氟烷麻醉后,采用脉冲波多普勒和组织多普勒成像分别检测二尖瓣舒张早期血液峰值速度(E)与二尖瓣环舒张早期运动速度(e'),以二者比值(E/e')反映左心室舒张功能;分别测量1.0%异氟烷麻醉下静息状态及2.5%异氟烷诱导充血状态下,冠状动脉舒张期血流峰值速度,以充血状态血流峰值速度/静息状态血流峰值速度为CFR。

1.6 小鼠心肌组织及细胞总RNA提取与RT-qPCR检测

采用RNA提取试剂盒提取组织和细胞总RNA,1 μg RNA经ABclonal反转录系统合成cDNA,用艾博泰克SYBR Green qPCR Master Mix进行定量检测,以GAPDH为内参,$2^{-\Delta\Delta Ct}$法计算目的基因相对表达量。

1.7 Western blotting检测小鼠心肌组织及HCMECs的细胞蛋白表达

RIPA裂解液提取总蛋白,BCA法测定蛋白浓度,SDS-PAGE电泳分离后转移至PVDF膜,封闭后与一抗4 ℃孵育过夜,一抗包括S100a6、β-catenin、TCF1、PARP9、STAT1、p-STAT1(稀释比均为1∶1 000)及GAPDH(1∶5 000)。荧光二抗室温孵育1 h,ECL化学发光显影,使用Image J进行定量分析。

1.8 免疫荧光染色检测目的分子的原位表达

采用酪酰胺信号放大(tyramide signal amplification,TSA)荧光系统进行免疫荧光染色。细胞或心脏组织切片经4%多聚甲醛固定30 min、0.3% Triton X-100室温通透15 min、5%牛血清白蛋白室温封闭1 h后,加入相应一抗(抗S100a6、PARP9、p-STAT1、β-catenin或CD31抗体,稀释比为1∶200),4 ℃孵育过夜。次日,辣根过氧化物酶(horseradish peroxidase,HRP)偶联二抗(1∶500)室温孵育1 h,用TSA工作液避光孵育10 min,DAPI染核5 min。用抗荧光淬灭剂进行封片,封片后激光共聚焦显微镜采集图像,采用Image J软件进行共定位,Pearson相关系数进行定量分析。

1.9 免疫共沉淀法检测蛋白相互作用

收集HG组和HG+siS100a6组细胞,预冷NP40裂解液(含1%蛋白酶抑制剂混合物、1%磷酸酶抑制剂)冰上裂解30 min,以4 ℃、12 000 r/min离心15 min,取上清。BCA法测定蛋白浓度后,取等量蛋白裂解液,加入抗β-catenin抗体或兔IgG对照抗体,4 ℃缓慢旋转孵育过夜。次日加入蛋白A/G磁珠,4 ℃孵育3 h。用磁力架磁性分离后收集免疫复合物,预冷NP40裂解液洗涤3次(每次5 min),加入(2×)上样缓冲液,100 ℃煮沸5 min。Western blotting检测TCF1蛋白表达,其中的Input组(总蛋白裂解液)作为阳性对照。

1.10 染色质免疫共沉淀检测TCF1与PARP9启动子区域的结合

参照SimpleChIP™试剂盒标准流程进行染色质免疫共沉淀实验。收集HG组和HG+siS100a6组细胞,1%甲醛室温交联10 min,甘氨酸终止交联。PBS洗涤后,裂解缓冲液A冰上裂解10 min,于4 ℃、3 000 r/min条件下离心沉淀细胞核5 min,裂解缓冲液B重悬后再次以4 ℃、3 000 r/min离心5 min,微球菌核酸酶37 ℃酶切20 min(0.5 μL/4×10^6个细胞),EDTA终止消化。染色质免疫沉淀缓冲液重悬后超声破碎(功率30%~40%,每次20 s,间隔30 s,共3次),以4 ℃、10 000 r/min离心10 min后取上清即为交联染色质。取其中的50 μL作为2% Input组,余液分别加入抗TCF1抗体(2 μg)或兔IgG,4 ℃旋转孵育过夜。加入蛋白G磁珠(30 μL),4 ℃孵育2 h;磁珠洗涤后,ChIP洗脱缓冲液65 ℃振荡洗脱30 min。解交联2 h后DNA纯化柱纯化,RT-qPCR检测PARP9启动子区TCF1结合位点富集情况,以Input为参照,根据$2^{-\Delta\Delta Ct}$法计算富集倍数。

1.11 S100a6与β-catenin/TCF1复合体分子对接预测

从蛋白质数据库(Protein Data Bank,PDB)获取S100a6(PDB ID:1K9K)和β-catenin/TCF1复合体(PDB

ID: 2Z6H)晶体结构。使用AutoDock Tools软件处理蛋白结构:去除水分子及杂原子,为S100a6添加极性氢原子并计算Gasteiger电荷,将β-catenin/TCF1复合体定义为受体并设置搜索格点。采用AutoDock Vina软件进行分子对接,以β-catenin与TCF1结合界面为中心设置搜索空间(60 Å×60 Å×60 Å),格点间距0.375 Å,运行次数100次,选取结合自由能最低构象作为最优结合模式。使用PyMOL软件进行三维可视化分析,预测S100a6与β-catenin/TCF1复合体的结合亲和力、关键结合界面及界面氨基酸残基相互作用类型。

1.12 细胞增殖实验检测HCMECs增殖能力

将HCMECs中加入终浓度为10 μmol/L的EdU试剂,置于37 ℃、5%CO_2培养箱中避光孵育2 h。随后弃去培养液,经4% 多聚甲醛固定、0.5%Triton X-100通透处理后,按照试剂盒说明书进行Click-iT反应。最后用DAPI进行细胞核染色,在荧光显微镜下随机选取视野拍照,采用Image J软件计数EdU阳性细胞数与总细胞数,计算EdU阳性细胞比例以反映细胞增殖能力。

1.13 划痕愈合实检测HCMECs迁移能力

采用划痕愈合实验评估HCMECs迁移能力。将细胞接种于培养板,常规培养至汇合度达90%时,用无菌200 μL移液管枪头在细胞单层均匀制造垂直划痕,PBS轻柔冲洗3次以去除脱落细胞,更换无血清培养基继续培养。分别于划痕后0、24 h在相同位置采集图像,采用Image J软件测量划痕宽度,计算划痕愈合率,以此评估细胞迁移能力。

1.14 成管实验检测HCMECs成管能力

采用基质胶成管实验检测HCMECs血管生成能力。取预冷的24孔细胞培养板,每孔加入Matrigel基质胶,置于37 ℃培养箱中孵育30 min使基质胶充分聚合。将各组HCMECs消化重悬后接种于基质胶上,置于37 ℃、5%CO_2培养箱中培养。培养结束后在显微镜下采集图像,采用Image J软件对小管分支点数进行定量分析,以评估细胞成管能力。

1.15 统计学分析

计量资料以$\bar{x}\pm s$表示;所有数据采用GraphPad Prism 9.0软件进行处理与分析,结果以可视化图表形式呈现,多组间连续变量比较采用单因素方差分析(One-way ANOVA),组间两两比较辅以Tukey事后检验,两组间差异评估采用双尾Student's t检验,以$P<0.05$为差异具有统计学意义。

2 结果

2.1 S100a6在CMD小鼠心脏内皮细胞中显著上调

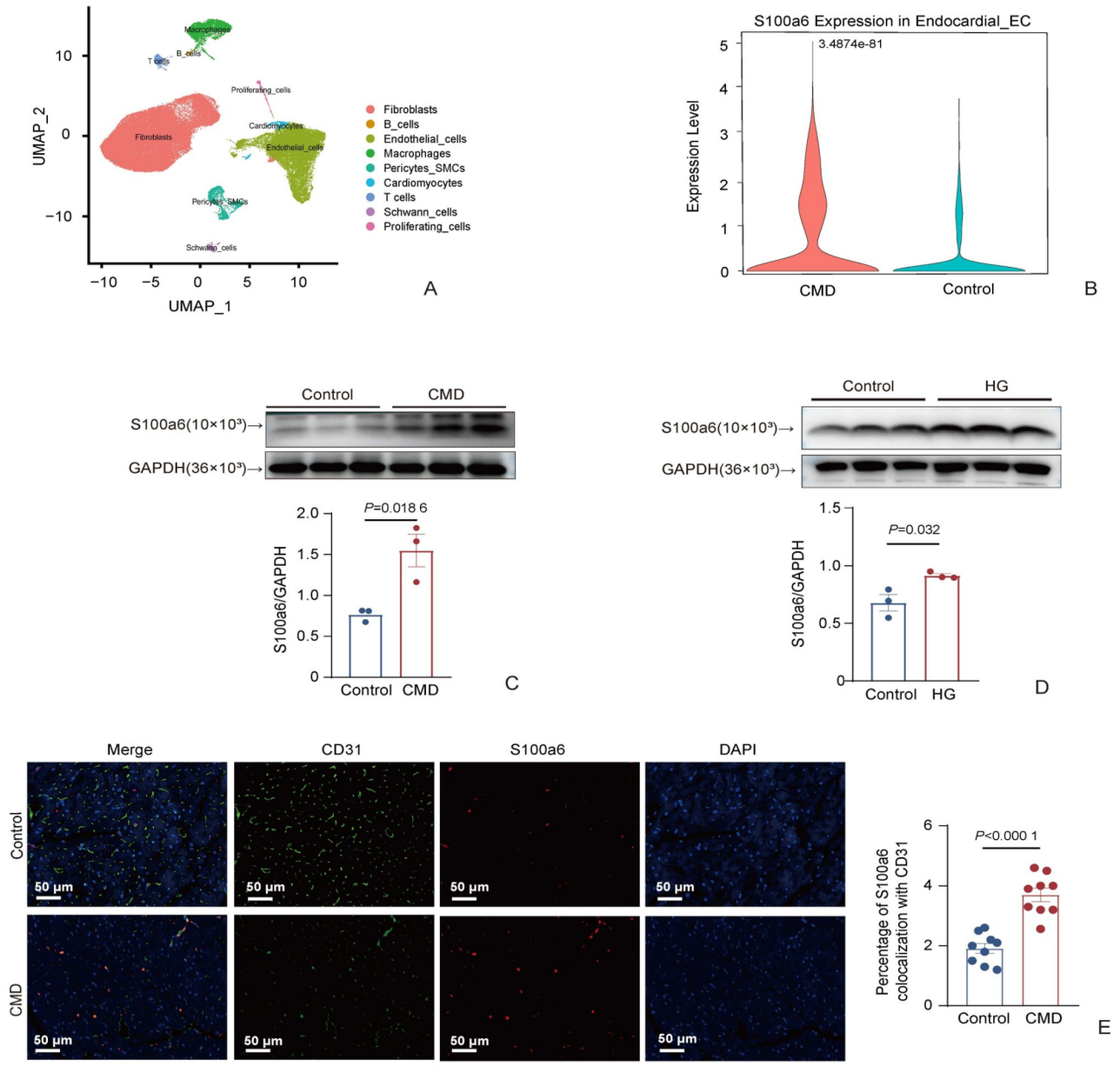
本研究采用单细胞RNA测序、Western blotting及免疫荧光共定位实验,检测小鼠心脏组织中S100a6的表达水平与细胞定位。与Control组小鼠相比,CMD组小鼠心脏组织的内皮细胞亚群中S100a6显著升高(图1A、B);Western blotting检测显示,CMD组小鼠心脏组织S100a6的蛋白表达水平均显著高于Control组($P<0.05$,图1C)。体外高糖联合游离脂肪酸处理HCMECs 48 h后,HG组S100a6蛋白表达水平显著高于Control组($P<0.05$,图1D);免疫荧光共定位结果显示,与Control组比较,CMD组小鼠心脏组织中S100a6与内皮标志物CD31的共定位信号明显增强($P<0.000\ 1$,图1E)。上述结果提示,S100a6在CMD小鼠心脏微血管内皮细胞中呈特异性高表达,可能参与冠状动脉微循环障碍的病理进程。

2.2 S100a6缺失加重CMD和HCMECs损伤

本研究采用超声心动图检测小鼠CFR及E/e′,免疫荧光染色检测心肌微血管密度,体外细胞功能实验(成管实验、划痕愈合实验、EdU增殖实验)检测HCMEC的成管、迁移及增殖能力。超声心动图结果显示,CMD-S100a6KD组小鼠的CFR显著低于Control组和CMD组($P<0.05$,图2A)。同时,舒张功能指标E/e'比值在CMD-S100a6KD组显著升高($P<0.05$,图2B)。在组织学层面,免疫荧光染色结果显示,与Control组相比,CMD组心肌微血管密度显著下降,CMD-S100a6 KD组微血管密度则较CMD组进一步降低($P<0.05$,图2C)。在细胞水平上,体外实验结果与体内表型高度一致,HG组HCMECs的成管能力(表现为分支数显著减少)、迁移能力(划痕愈合率显著降低)和增殖能力(EdU阳性率显著降低)均显著低于Control组,而HG+siS100a6组则较HG+siNC组进一步下降($P<0.05$,图2D~F)。上述结果提示,S100a6缺失可显著加重CMD小鼠冠状动脉微循环障碍、舒张功能障碍及心肌微血管损伤,并损害HCMECs的血管生成、迁移和增殖能力,表明S100a6在维持心脏微血管内皮细胞功能稳态中发挥重要保护作用。

2.3 S100a6缺失可导致PARP9上调激活STAT1信号通路

本研究对HG处理的HCMECs(HG+siNC组和HG+siS100a6组)进行批量RNA测序、RT-qPCR、

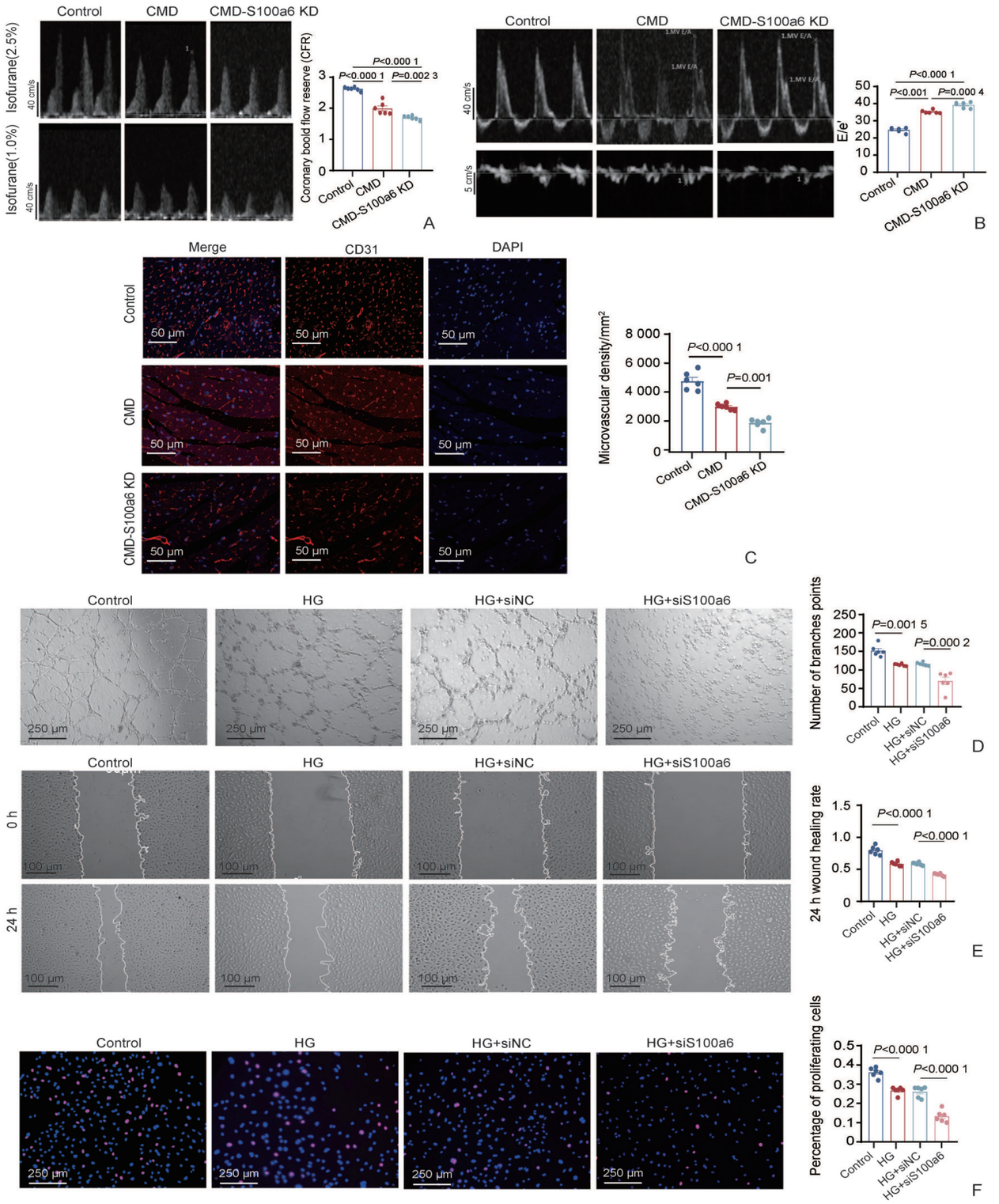


A: UMAP clustering analysis of major cell subpopulations in cardiac tissues; B: Violin plot of S100a6 expression levels in endothelial cell subpopulations; C: Protein expression and quantitative statistics of S100a6 in cardiac tissues; D: Protein expression and quantitative statistics of S100a6 in HCMECs; E: Colocalization expression and quantitative analysis of S100a6 and CD31 in cardiac tissues

图1 S100a6在CMD小鼠模型及细胞模型中的表达上调

Figure 1 Upregulation of S100a6 expression in CMD mouse model and cell model

Western blotting、免疫荧光及细胞功能实验对相关分子表达及细胞功能进行检测。批量RNA测序结果显示,S100a6敲低后,*PARP9*基因表达显著上调,GO富集分析进一步揭示,STAT1信号通路在S100a6敲低后显著富集(图3A),并通过RT-qPCR验证了HG+siS100a6组*PARP9*的mRNA水平较HG+siNC组显著升高($P<0.05$,图3B)。为了明确PARP9在S100a6缺失诱导的STAT1激活中的作用,在S100a6敲低的同时沉默PARP9,结果显示,HG+siS100a6+siPARP9组的STAT1磷酸化(p-STAT1)水平较HG+siS100a6组显著降低($P<0.000\,1$,图3C)。功能学实验证实,沉默PARP9显著改善了S100a6敲低引起的HCMECs的成管、迁移和增殖缺陷($P<0.05$,图3D~F)。上述结果提示,S100a6缺失可通过上调PARP9进而激活STAT1信号通路,从而介导



A and B: Representative echocardiograms and quantitative analysis of coronary flow reserve (CFR), diastolic function index (E/e') in mice of the Control group, CMD group and CMD-S100a6 KD group; C: Representative immunofluorescence images and quantitative analysis of myocardial microvessel density (CD31-positive) in each group; D: Representative images and quantitative statistics of tube formation assays in HCMECs of each group; E: Representative images and quantitative analysis of scratch wound healing assays in HCMECs of each group; F: Representative images and quantitative analysis of EdU cell proliferation assays and positive cell rate in each group

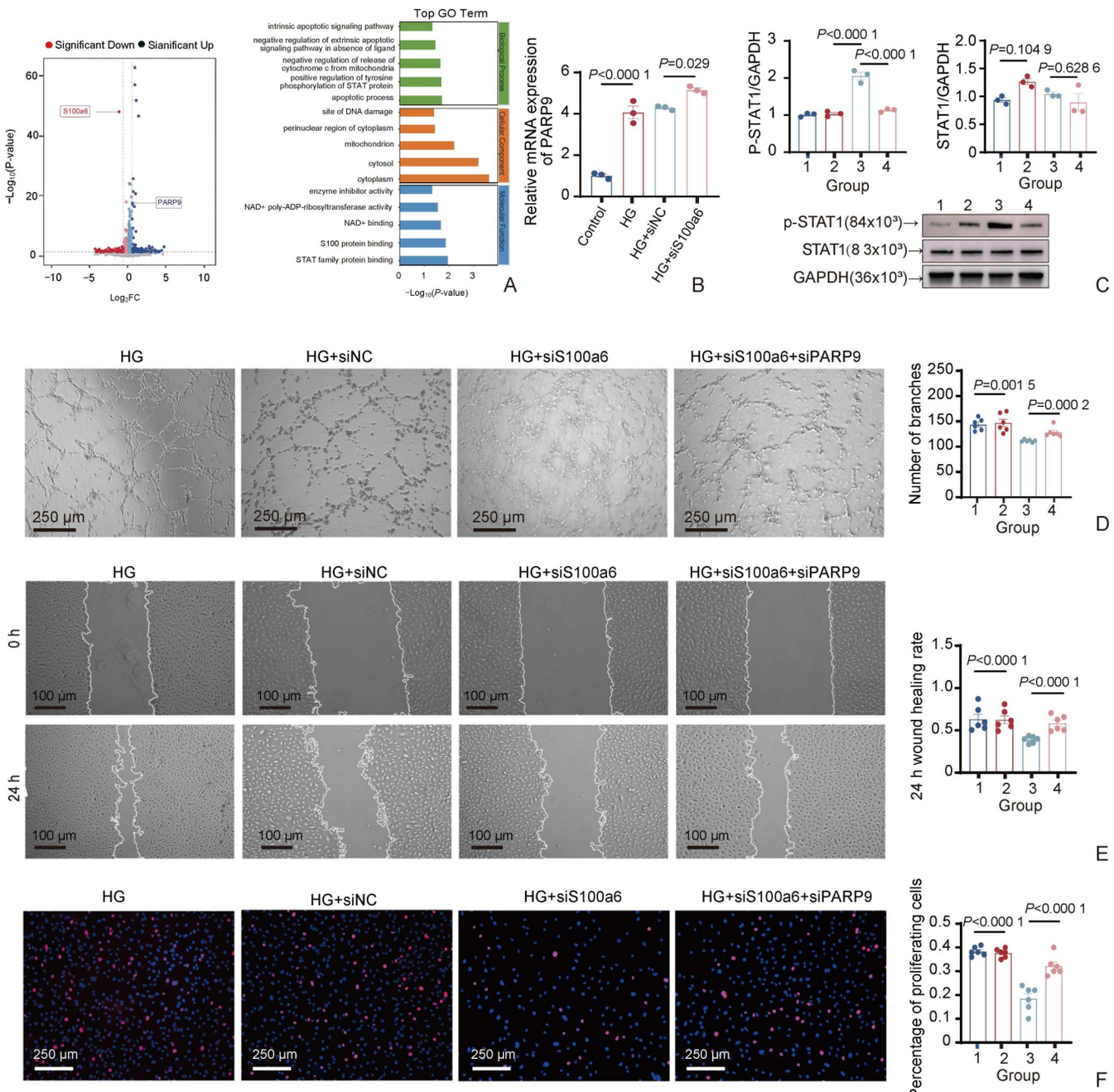
图2 敲低S100a6加重小鼠冠状动脉微循环障碍及HCMECs功能损伤

Figure 2 Knockdown of S100a6 exacerbates coronary microcirculation disturbance in CMD mice and functional injury in HCMECs

HCMECs功能障碍，而靶向抑制PARP9可有效逆转该损伤效应，表明PARP9/STAT1信号轴是S100a6发挥心脏微血管内皮细胞保护作用的重要下游机制。

2.4　S100a6稳定β-catenin/TCF1复合体抑制PARP9转录

本研究采用RT-qPCR、Western blotting、免疫共沉淀、染色质免疫共沉淀及分子对接预测等方法，检测



A: Volcano plot of differentially expressed genes and GO biological process enrichment analysis between HG+si-NC and HG+si-S100a6 groups; B: Detection of PARP9 mRNA expression in HCMECs among different treatments; C: Representative blots and quantitative analysis of p-STAT1 and total STAT1 in HCMECs under different treatments; D: Representative images and quantitative analysis of tube formation and branch number of HCMECs in each group; E: Representative images and quantitative analysis of scratch wound healing rate of HCMECs in each group; F: Representative images and quantitative analysis of cell positive rate in EdU proliferation assay of each group. 1: HG group; 2: HG+siNC group; 3: HG+siS100a6 group; 4: HG+siS100a6+siPARP9 group

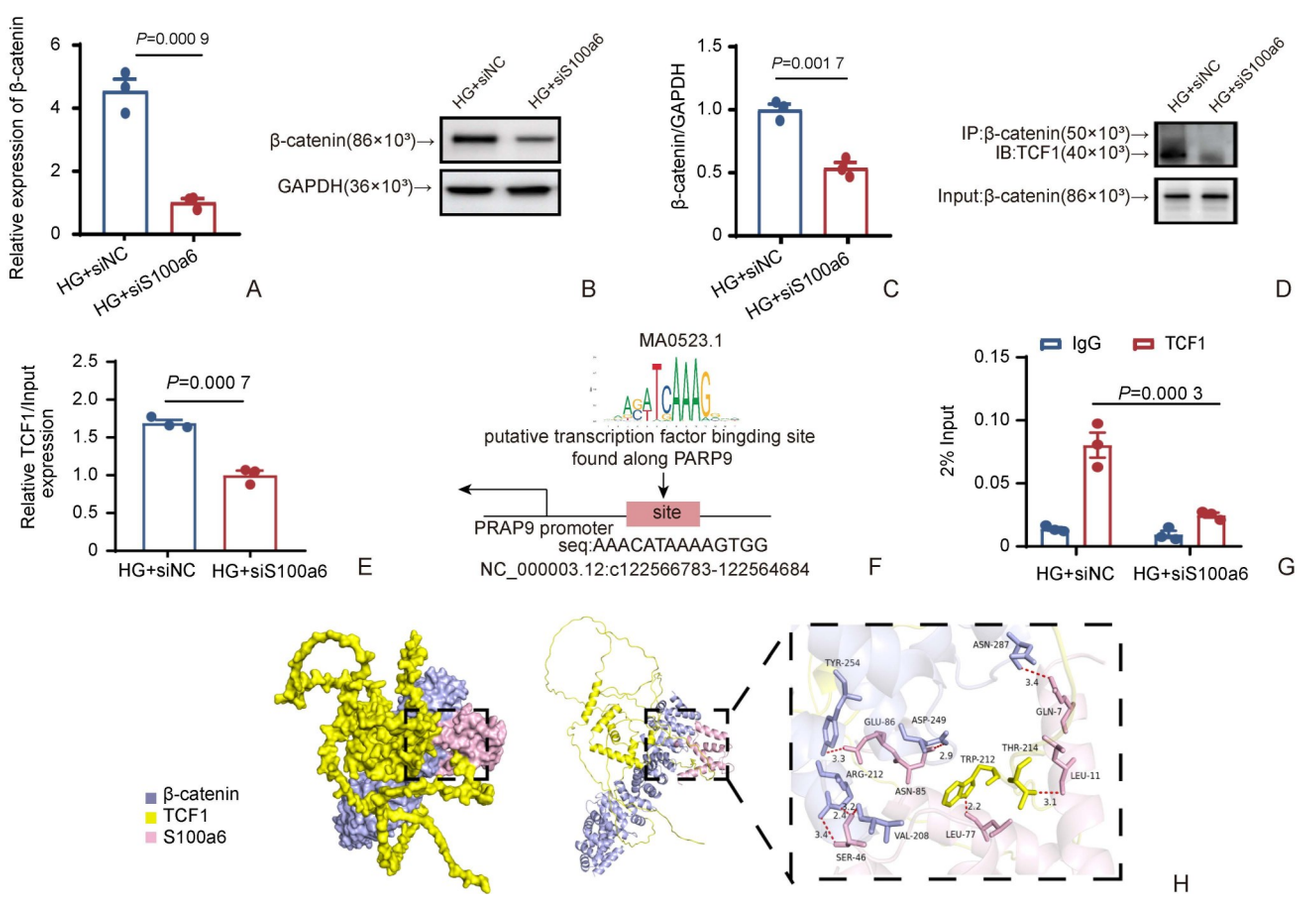
图3　S100a6缺失通过上调PARP9激活STAT1信号通路加重HCMECs功能障碍

Figure 3　Aggravation of HCMECs dysfunction by S100a6 deficiency *via* PARP9/STAT1 pathway

S100a6对Wnt/β-catenin信号通路及β-catenin/TCF1复合体形成的影响。RT-qPCR和Western blotting结果一致显示,与HG+siNC组比较,HG+siS100a6组中,β-catenin的mRNA和蛋白水平均显著降低($P<0.05$,图4A~C)。为进一步探究S100a6与β-catenin/TCF1复合体的直接关系,进行了免疫共沉淀实验,结果显示,S100a6敲低显著减弱了β-catenin与TCF1的相互作用($P<0.05$,图4D、E)。随后,通过ChIP实验,检测了β-catenin/TCF1复合体对*PARP9*启动子的结合情况。结果证实,在S100a6缺失的细胞中,β-catenin/TCF1复合体与*PARP9*启动子区域的结合显著减少($P<0.05$,图4F、G)。此外,分子对接预测分析发现S100a6巧妙地"跨坐"在TCF1和β-catenin的结合界面缝隙中,通过多点锚定效应稳定了三元结构,为S100a6直接参与该复合体的调控提供了结构基础(图4H)。上述结果提示,S100a6可通过稳定β-catenin/TCF1复合体,增强其与*PARP9*启动子的结合,从而抑制PARP9转录。

2.5　过表达β-catenin挽救S100a6缺失诱导的内皮细胞功能障碍

为确证S100a6通过β-catenin/TCF1复合体调控PARP9的分子轴线,本研究在S100a6沉默的HCMECs中过表达β-catenin,采用Western blotting及细胞功能实验(成管实验、划痕愈合实验、EdU增殖实验)检测PARP9/STAT1信号轴及内皮细胞功能的变化。结果显示,β-catenin过表达显著逆转了S100a6敲低引起的PARP9蛋白水平的上调($P<0.05$,图5A),这一分子层面的回复效应进一步向下游传递,导致p-STAT1蛋白水平显著下降($P<0.05$,图5B)。在功能学层面,β-catenin过表达显著改善了HG+siS100a6组HCMECs的成管分

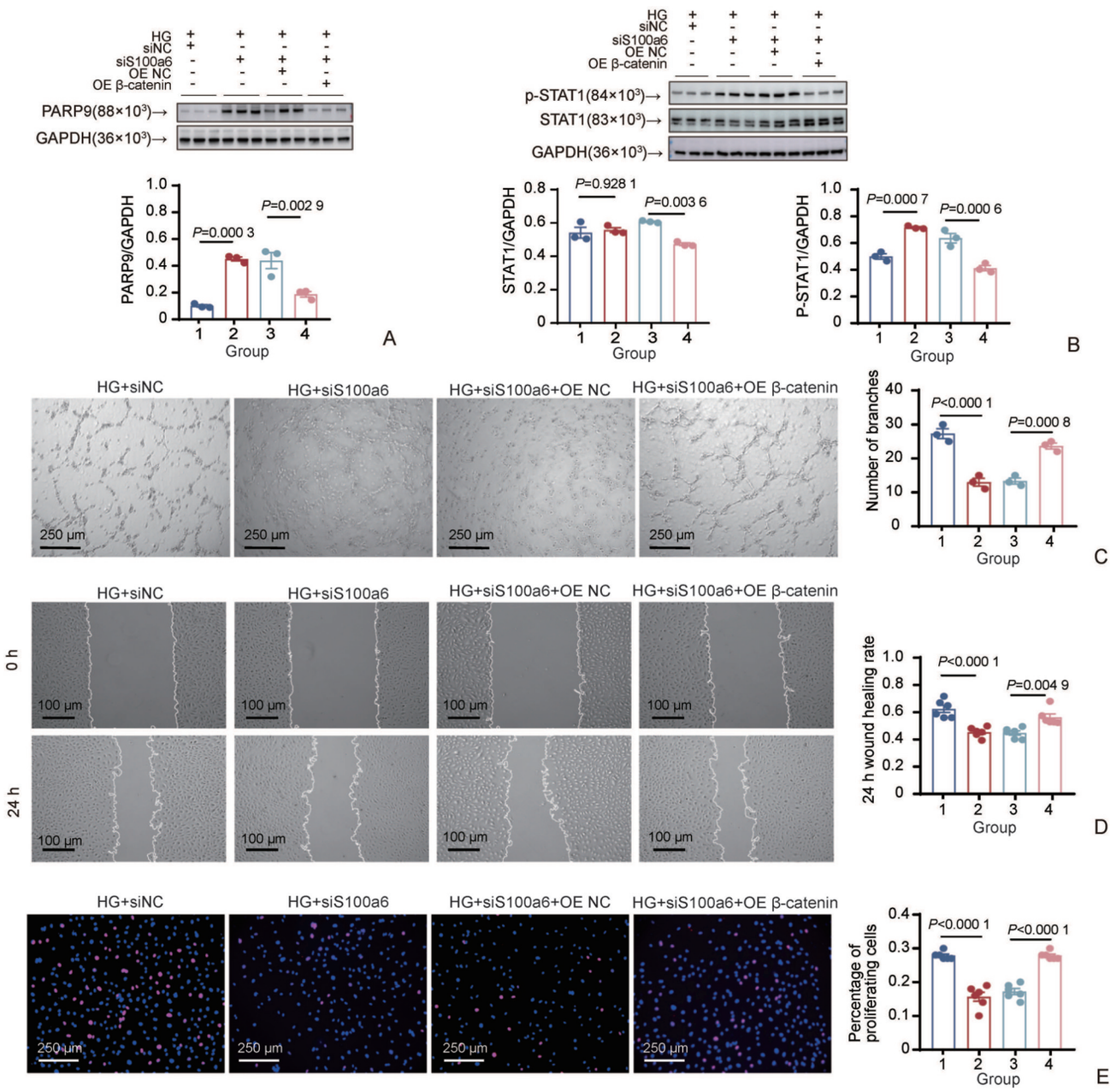


A: Relative mRNA expression levels of β-catenin in HCMECs of HG+siNC and HG+siS100a6 groups; B and C: Representative Western blot bands and quantitative analysis of β-catenin protein expression in the two groups; D and E: Electrophoretic bands and quantitative statistics of Co-IP assay for verifying the interaction between β-catenin and TCF1 proteins; F: Schematic diagram of the predicted TCF1 binding motif (MA0523.1) in the promoter region of *PARP9* gene; G: Binding capacity of TCF1 to the PARP9 promoter in HCMECs of HG+siNC and HG+siS100a6 groups; H: Molecular docking simulation diagram of the ternary complex composed of S100a6, β-catenin and TCF1

图4　S100a6敲低对β-catenin/TCF1复合体及PARP9转录的调控作用

Figure 4　Regulation of β-catenin/TCF1 complex and PARP9 transcription in S100a6 knockdown

支数、划痕愈合率和增殖细胞比例($P<0.05$,图5C~E)。上述结果提示,过表达β-catenin可有效挽救S100a6缺失诱导的PARP9上调及STAT1信号通路过度激活,进而恢复HCMECs的血管生成、迁移和增殖能力,进一步证实S100a6通过β-catenin/TCF1/PARP9/STAT1信号轴发挥心脏微血管内皮细胞保护作用。



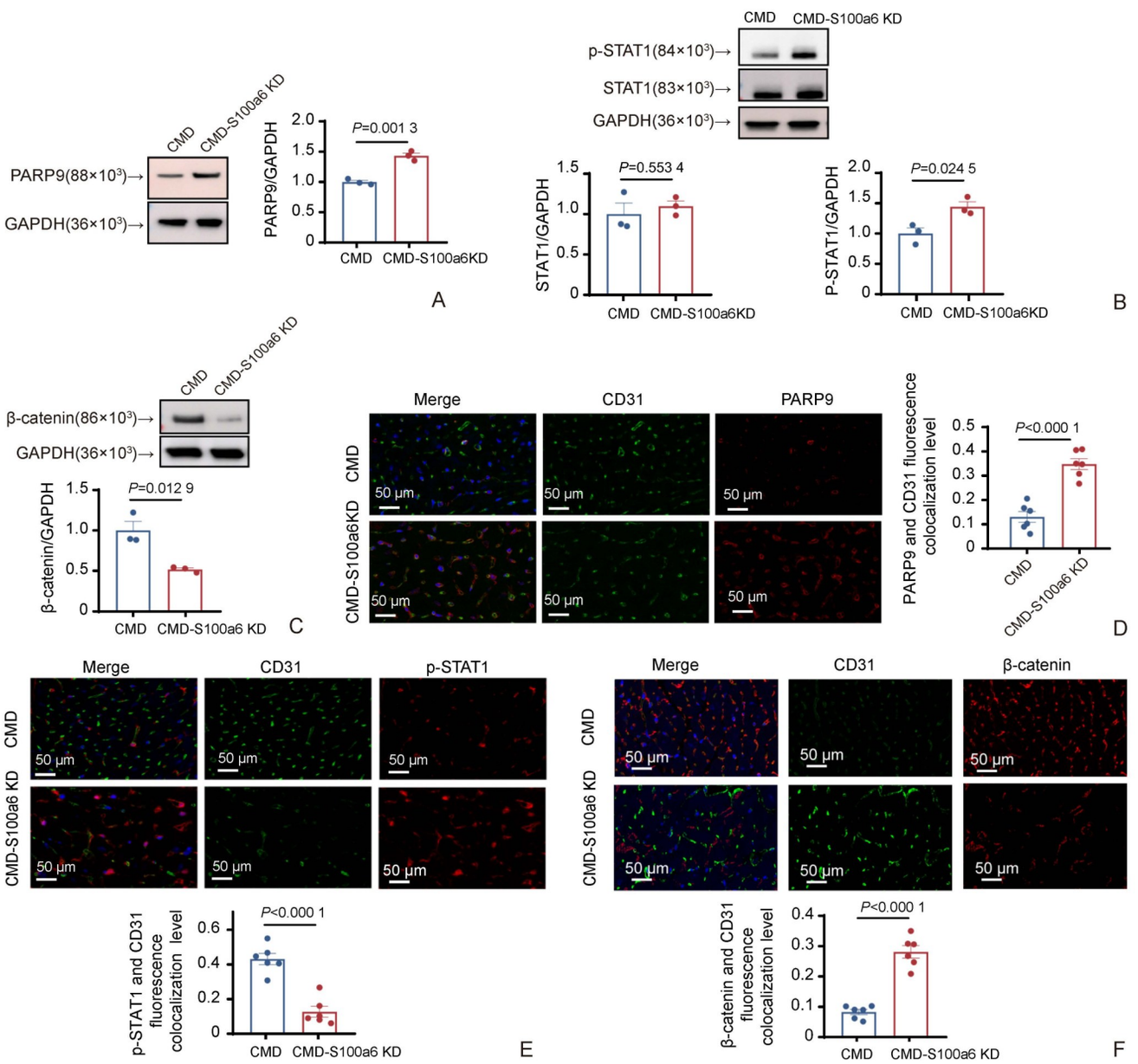
A: Representative Western blot bands and quantitative analysis of PARP9 protein expression in HCMECs of each group; B: Representative Western blot bands and quantitative analysis of p-STAT1 and total STAT1 protein expression in HCMECs of each group; C: Representative images of angiogenesis assay and quantitative analysis of tube branch number in HCMECs of each group; D: Representative images of scratch wound healing assay and quantitative analysis of wound healing rate in HCMECs of each group; E: Representative images of EdU proliferation assay and quantitative analysis of positive cell rate in HCMECs of each group. 1: HG+siNC group; 2: HG+siS100a6 group; 3: HG+siS100a6+OE NC group; 4: HG+siS100a6+OE β-catenin group

图5 β-catenin过表达对S100a6缺失所致HCMECs功能障碍及PARP9/STAT1信号激活的挽救效应

Figure 5 Rescue effect of β-catenin overexpression in HCMECs dysfunction and excessive activation of PARP9/STAT1 signaling axis induced by S100a6 deficiency

2.6　体内验证S100a6/β-catenin/PARP9/STAT1轴调控关系

为在体内验证S100a6对β-catenin/PARP9/STAT1信号轴的调控关系,本研究采用免疫荧光染色及Western blotting等方法检测CMD-S100a6 KD组小鼠心脏组织中各分子的表达变化及内皮细胞定位。结果显示:CMD-S100a6 KD组小鼠心脏组织中PARP9的蛋白水平较CMD组显著升高($P<0.05$,图6A)。伴随着PARP9的升高,下游STAT1信号通路也被激活。与CMD组比较,CMD-S100a6 KD组小鼠心脏组织中p-STAT1蛋白水平显著升高($P<0.05$,图6B)。作为上游核心调控因子,CMD-S100a6 KD组小鼠心脏组织中β-catenin



A: Representative Western blot bands and quantitative analysis of PARP9 protein in cardiac tissues; B: Representative Western blot bands and quantitative analysis of STAT1 and p-STAT1 protein in cardiac tissues; C: Representative Western blot bands and quantitative analysis of β-catenin protein in cardiac tissues; D: Representative immunofluorescence images and Pearson correlation coefficient analysis of PARP9 and CD31 colocalization in cardiac tissues; E: Representative immunofluorescence images and Pearson correlation coefficient analysis of p-STAT1 and CD31 colocalization in cardiac tissues; F: Representative immunofluorescence images and Pearson correlation coefficient analysis of β-catenin and CD31 colocalization in cardiac tissues

图6　S100a6缺失介导CMD小鼠心脏微血管损伤及通路分子表达变化

Figure 6　Changes in cardiac microvascular injury and pathway molecule expression induced by S100a6 deficiency in CMD mice

的蛋白表达也较CMD组显著降低(P<0.05,图6C)。免疫荧光进一步显示各分子在内皮细胞中的定位变化:与CMD组比较,CMD-S100a6KD组PARP9与CD31的共定位显著增强(P<0.05,图6D),p-STAT1与CD31的共定位显著增强(P<0.05,图6E),而β-catenin与CD31的共定位显著减少(P<0.05,图6F)。这些结果提示,S100a6敲低后PARP9/STAT1通路激活,同时β-catenin表达下调。上述结果提示,在体内S100a6缺失可导致β-catenin表达下调,进而解除对PARP9的转录抑制并激活下游STAT1信号通路,最终介导心脏微血管内皮细胞功能障碍,进一步证实S100a6/β-catenin/PARP9/STAT1信号轴在CMD病理进程中发挥关键的调控作用。

3 讨论

本研究揭示了S100a6在CMD中的保护性作用,发现其在CMD小鼠的冠状动脉微血管内皮中呈现代偿性上调,并通过单细胞转录组学、基因遗传学操作及分子生物学等手段证明了S100a6是维持血管内皮稳态的关键分子。在机制上,本研究证实S100a6可通过物理结合并稳定β-catenin/TCF1复合体,维持该复合体在PARP9启动子上的占据以抑制PARP9的转录,进而限制STAT1信号通路激活,维持冠状动脉微血管内皮细胞稳态,S100a6的缺失破坏了这一稳态,导致冠状动脉微血管内皮细胞增殖、成管、迁移能力受损(图7),这一发现为CMD的治疗提供了新的分子靶点。

3.1 S100a6作为CMD的代偿性保护因子

S100a6作为S100钙结合蛋白家族的一员,在心血管病理中的确切作用长期未有定论。既往观点倾向于将其视为细胞应激或损伤的标志分子。有研究观察到急性冠脉综合征(acute coronary syndrome,ACS)患者血清S100a6水平升高,但在该研究中将其归因为细胞膜破裂后的蛋白渗漏,是反映组织损伤程度的生物标志物[12]。然而,也有学者指出S100a6可能具有保护作用,在心肌细胞中S100a6可通过调节p53的磷酸化状态来抑制细胞凋亡,从而减轻缺血/再灌注损伤[13-14,18]。更重要的是,研究发现S100a6是内皮细胞周期进程的关键调节因子,其缺失会导致内皮细胞增殖停滞[19]。尽管这些研究提示了S100a6的细胞保护潜力,但其在CMD这一特定病理环境下的功能仍属空白,特别是在代谢紊乱引发的慢性微血管稀疏化过程中,内源性S100a6究竟是促进了内皮损伤,还是代偿性升高,并未被阐明。本研究创新性发现S100a6可作为CMD的代偿性保护因子,并发现在代谢性CMD模型中,冠状动脉微血管内皮细胞特异性地发生了S100a6转录水平的显著上调,与“损伤标志物”假说截然不同,本研究中的功能缺失实验提供了决定性证据:当特异性敲低内皮S100a6后,微血管内皮并未因“致病因子”的去除而获益,反而表现出更加严重的内皮细胞功能障碍,导致活体水平上CFR的进一步降低。这一结果有力地证明,在CMD的早期或进展阶段,微血管内皮系统启动了S100a6的表达上调,是一种适应性的、旨在维持内皮稳态的代偿性保护反应。

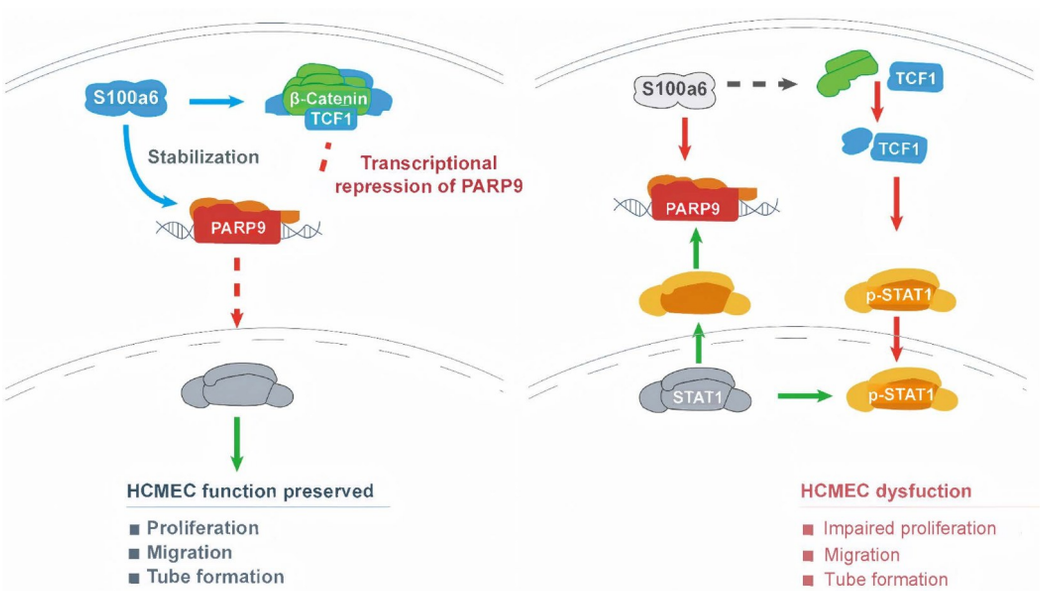


图7 S100a6在冠状动脉微循环障碍中的保护机制示意图

Figure 7 Schematic diagram illustrating the protective mechanism of S100a6 against coronary microvascular dysfunction

这种内源性防御机制的发现,不仅重新定义了S100a6在CMD病理中的生物学属性,也解释了为何单纯针对代谢指标的控制往往难以完全逆转微血管损伤——因为维持微血管完整性的内源性S100a6可能已耗竭或功能失调。

3.2 S100a6可通过稳定β-catenin/TCF1复合体发挥转录抑制调控作用

S100a6作为钙结合蛋白,其构象变化高度依赖胞内Ca^{2+}浓度,这种特性为其与靶蛋白的互作奠定了结构基础。已有研究证实,在肿瘤和心肌细胞中,S100a6可通过与p53、ANXA11等蛋白结合,调控细胞凋亡和耐药性[14,20],提示其功能发挥具有显著的"互作蛋白依赖性"。此外,前期研究提示S100a6与Wnt/β-catenin信号通路存在潜在关联[21],但该研究并未阐明二者的作用方式,本研究提示S100a6在微血管内皮细胞中与β-catenin/TCF1转录复合体的结合。Wnt/β-catenin信号通路在血管稳态维持中扮演着重要角色[22],其转录输出很大程度上取决于β-catenin与特定共转录因子(如TCF/LEF家族)的招募情况[23-25]。免疫共沉淀和功能缺失实验表明,S100a6充当了β-catenin/TCF1复合体的"分子伴侣"或"稳定剂",染色质免疫共沉淀实验分析进一步阐明了该复合体的下游效应:β-catenin/TCF1复合体特异性结合于*PARP9*基因启动子区域,发挥转录抑制作用,当S100a6缺失时,β-catenin/TCF1复合体稳定性下降,导致TCF1从*PARP9*启动子上解离,从而解除了对*PARP9*的转录抑制,引发其表达上调。这一发现不仅揭示了S100a6维持微血管内皮稳态的分子机制,也丰富了对Wnt信号在血管病理中非经典转录调控模式的理解。

3.3 PARP9是连接S100a6缺乏与STAT1信号激活的关键介质

在该信号轴的下游,本研究鉴定出PARP9是介导内皮损伤的关键效应分子。PARP9作为非经典PARP家族成员,参与炎症和缺血损伤,其与STAT1信号通路的调控关系已有广泛报道[19]。本研究发现S100a6缺失引发的PARP9异常上调,直接导致了STAT1的磷酸化激活及其核转位增加。功能性回复实验进一步确立了PARP9在微血管稀疏化过程中的作用,特异性敲低PARP9可显著逆转由S100a6缺失诱导的内皮细胞增殖停滞和成管缺陷。此外,通过过表达β-catenin抑制PARP9的转录水平,同样能够恢复正常的STAT1信号状态,从而完整验证了S100a6/β-catenin/PARP9/STAT1这一级联调控轴。这一发现不仅明确了PARP9在CMD中的致病作用,也完善了关于S100a6调控内皮细胞周期的机制,填补了连接S100a6缺失与STAT1激活之间的关键分子缺口。

本研究仍存在一定局限性。首先,本研究仅采用ob/ob小鼠构建代谢性CMD模型,难以完全模拟临床CMD复杂的病理生理状态。其次,实验仅在雄性ob/ob小鼠中开展,未纳入雌性个体,后续有必要引入雌性动物,进一步探究雌激素对CMD表型的保护作用及潜在的性别差异机制。最后,S100a6的保护作用仅在当前单一模型中得到验证,仍需在高脂饮食诱导、STZ诱导等多种CMD动物模型中开展后续验证。

目前临床针对CMD缺乏特异性治疗手段,仍以血糖、血压等传统危险因素的常规管控为主[2]。本研究揭示了S100a6是维持冠状动脉微血管内皮结构与功能稳态的关键内源性保护分子,提示稳定或上调内皮S100a6表达有望成为CMD防治的潜在新思路。参照维生素D类似物在糖尿病肾病中的靶向应用模式[26],未来研发S100a6小分子激动剂或PARP9特异性抑制剂,可为冠状动脉微循环障碍的精准治疗提供新方向。

利益冲突 本文所有作者声明不存在利益冲突

参考文献:

[1] NAGHAVI M, ONG K L, AALI A, *et al*. Global burden of 288 causes of death and life expectancy decomposition in 204 countries and territories and 811 subnational locations, 1990—2021: a systematic analysis for the Global Burden of Disease Study 2021[J]. Lancet, 2024, 403(10440): 2100-2132. DOI:10.1016/S0140-6736(24)00367-2.

[2] DEL BUONO M G, MONTONE R A, CAMILLI M, *et al*. Coronary microvascular dysfunction across the spectrum of cardiovascular diseases JACC state-of-the-art review[J]. J Am Coll Cardiol, 2021, 78(13): 1352-1371. DOI:10.1016/j.jacc.2021.07.042.

[3] SUDA A, TAKAHASHI J, HAO K, *et al*. Coronary functional abnormalities in patients with angina and nonobstructive coronary artery disease[J]. J Am Coll Cardiol, 2019, 74(19): 2350-2360. DOI: 10.1016/j.jacc.2019.08.1056.

[4] ROUAULT P, GUIMBAL S, CORNUAULT L, *et al*. Thrombosis in the coronary microvasculature impairs cardiac relaxation and induces diastolic dysfunction[J]. Arterioscler Thromb Vasc Biol, 2024, 44(1): e1-e18. DOI: 10.1161/atvbaha.123.320040.

[5] CHEN Y Q, LI S, GUAN B, *et al*. MAP4K4 exacerbates cardiac microvascular injury in diabetes by facilitating snitrosylation modification of Drp1[J]. Cardiovasc Diabetol, 2024, 23(1): 164. DOI:10.1186/s12933-024-02254-7.

[6] SI R, ZHANG Q, TSUJI-HOSOKAWA A, *et al*. Overexpression of p53 due to excess protein O-GlcNAcylation is associated with coronary microvascular disease in type 2

diabetes[J]. Cardiovasc Res, 2020, 116(6): 1186-1198. DOI:10.1093/cvr/cvz216.

[7] WANG X Y, WANG X T, ZHUANG H, *et al*. A GLP-1 receptor agonist semaglutide attenuates cardiac microvascular injury in HFD/STZ-induced diabetic mice [J]. Eur J Pharmacol, 2026, 1011: 178429. DOI: 10.1016/j. ejphar. 2025.178429.

[8] YANG Z H, LIU Y X, LI Z Z, *et al*. Coronary microvascular dysfunction and cardiovascular disease: pathogenesis, associations and treatment strategies [J]. Biomed Pharmacother, 2023, 164: 115011. DOI: 10.1016/j.biopha. 2023.115011.

[9] 林璐, 户丽君, 黄逸云, 等. S100A6通过招募和活化巨噬细胞促进血管形成[J]. 中国生物工程杂志, 2020, 40(5): 7-14. DOI:10.13523/j.cb.1910054.
LIN L, HU L J, HUANG Y Y, *et al*. S100A6 promotes angiogenesis through recruiting and activating macrophages [J]. China Biotechnol, 2020, 40(5): 7-14. DOI:10.13523/j. cb.1910054.

[10] WANG Y D, KANG X W, KANG X, *et al*. S100A6: molecular function and biomarker role [J]. Biomark Res, 2023, 11(1): 78. DOI:10.1186/s40364-023-00515-3.

[11] ZHOU Y, ZHA Y W, YANG Y Q, *et al*. S100 proteins in cardiovascular diseases[J]. Mol Med, 2023, 29(1): 68. DOI:10.1186/s10020-023-00662-1.

[12] CAI X Y, LU L, WANG Y N, *et al*. Association of increased S100B, S100A6 and S100P in serum levels with acute coronary syndrome and also with the severity of myocardial infarction in cardiac tissue of rat models with ischemia-reperfusion injury[J]. Atherosclerosis, 2011, 217(2): 536-542. DOI:10.1016/j.atherosclerosis. 2011. 05.023.

[13] MOFID A, NEWMAN N S, LEE P J H, *et al*. Cardiac overexpression of S100A6 attenuates cardiomyocyte apoptosis and reduces infarct size after myocardial ischemia-reperfusion[J]. J Am Heart Assoc, 2017, 6(2): e004738. DOI:10.1161/jaha.116.004738.

[14] TSOPORIS J N, IZHAR S, PARKER T G. Expression of S100A6 in cardiac myocytes limits apoptosis induced by tumor necrosis factor-α[J]. J Biol Chem, 2008, 283(44): 30174-30183. DOI:10.1074/jbc.M805318200.

[15] SOROP O, VAN DE WOUW J, CHANDLER S, *et al*. Experimental animal models of coronary microvascular dysfunction[J]. Cardiovasc Res, 2020, 116(4): 756-770. DOI:10.1093/cvr/cvaa002.

[16] WESTERGREN H U, GRÖNROS J, HEINONEN S E, *et al*. Impaired coronary and renal vascular function in spontaneously type 2 diabetic leptin-deficient mice [J]. PLoS One, 2015, 10(6): e0130648. DOI:10.1371/journal. pone.0130648.

[17] ADINGUPU D D, GÖPEL S O, GRÖNROS J, *et al*. SGLT2 inhibition with empagliflozin improves coronary microvascular function and cardiac contractility in prediabetic ob/ob$^{-/-}$ mice[J]. Cardiovasc Diabetol, 2019, 18(1): 16. DOI:10.1186/s12933-019-0820-6.

[18] TSOPORIS J T, IZHAR S, DESJARDINS J F, *et al*. Conditional cardiac overexpression of S100A6 attenuates myocyte hypertrophy and apoptosis following myocardial infarction[J]. Curr Pharm Des, 2014, 20(12): 1941-1949. DOI:10.2174/13816128113199990444.

[19] LERCHENMÜLLER C, HEIßENBERG J, DAMILANO F, *et al*. S100A6 regulates endothelial cell cycle progression by attenuating antiproliferative signal transducers and activators of transcription 1 signaling [J]. Arterioscler Thromb Vasc Biol, 2016, 36(9): 1854-1867. DOI: 10.1161/atvbaha.115.306415.

[20] 徐宁, 李勇. 膜联蛋白A11在肿瘤中的研究进展[J]. 现代医药卫生, 2024, 40(3): 472-476, 481.
XU N, LI Y. Research progress of annexin A11 in tumors [J]. J Mod Med Health, 2024, 40(3): 472-476, 481.

[21] TIAN H Z, PAN Q G, WU J F, *et al*. Icariin ameliorates Coxsackievirus B3-induced viral myocarditis by modulating the S100 calcium binding protein A6/β -catenin/c-Myc signaling pathway[J]. Phytomedicine, 2024, 135: 156214. DOI:10.1016/j.phymed.2024.156214.

[22] 王玉雯, 李芙蓉, 袁容娣. Gpr124对高糖环境下视网膜微血管内皮细胞增殖、迁移和血管形成的调控作用[J]. 陆军军医大学学报, 2024, 46(18): 2101-2109. DOI:10.16016/j.2097-0927.202403058.
WANG Y W, LI F R, YUAN R D. Regulatory effect of Gpr124 on proliferation, migration and angiogenesis of retinal microvascular endothelial cells under high-glucose condition[J]. J Army Med Univ, 2024, 46(18): 2101-2109. DOI:10.16016/j.2097-0927.202403058.

[23] HAYBAR H, KHODADI E, SHAHRABI S. Wnt/β-catenin in ischemic myocardium: interactions and signaling pathways as a therapeutic target[J]. Heart Fail Rev, 2019, 24(3): 411-419. DOI:10.1007/s10741-018-9759-z.

[24] JIANG L, YIN M, WEI X X, *et al*. Bach1 represses Wnt/β -catenin signaling and angiogenesis[J]. Circ Res, 2015, 117(4): 364-375. DOI:10.1161/circresaha.115.306829.

[25] GELFAND B D, MELLER J, PRYOR A W, *et al*. Hemodynamic activation of β -catenin and T-cell-specific transcription factor signaling in vascular endothelium regulates fibronectin expression [J]. Arterioscler Thromb Vasc Biol, 2011, 31(7): 1625-1633. DOI: 10.1161/atvbaha.111.227827.

[26] 张丰睿, 陈青松. 维生素D及其类似物治疗糖尿病肾病的研究进展[J]. 现代医药卫生, 2023, 39(9): 1539-1545. DOI:10.3969/j.issn.1009-5519.2023.09.021.
ZHANG F R, CHEN Q S. Therapeutic advances of vitamin D and its analogues in diabetic kidney disease[J]. J Mod Med Health, 2023, 39(9): 1539-1545. DOI: 10.3969/j. issn. 1009-5519.2023.09.021.

(收稿:2026-02-24;修回:2026-04-28)
(编辑 汤锦波)